

Synthesis and crystal structure of a ten-coordinate plutonium(IV) ion complexed by 2-[(diphenylphosphino)methyl]pyridine *N,P*-dioxide: $[\text{Pu}(\text{NO}_3)_3\{2\text{-}[(\text{C}_6\text{H}_5)_2\text{P}(\text{O})\text{CH}_2]\text{C}_5\text{H}_4\text{NO}\}_2]\text{-}[\text{Pu}(\text{NO}_3)_6]_{0.5}$

John H. Matonic,^a Mary P. Neu,^{*a} Alejandro E. Enriquez,^a Robert T. Paine^{*b} and Brian L. Scott^a

^a Chemical Science and Technology Division, Los Alamos National Laboratory, Los Alamos, NM 87545, USA. E-mail: mneu@lanl.gov

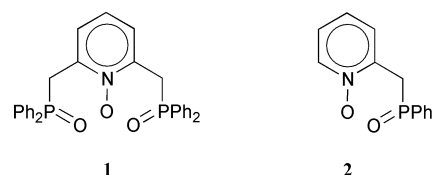
^b Department of Chemistry, University of New Mexico, Albuquerque, NM 87131, USA. E-mail: rpaine@unm.edu

Received 23rd July 2001, Accepted 11th March 2002

First published as an Advance Article on the web 24th April 2002

The bifunctional ligand 2-[(C₆H₅)₂P(O)CH₂]C₅H₄NO (**2**), in EtOH, combined in a 1 : 1 ratio with Pu(IV) in an aqueous nitric acid solution, produced an orange–brown coordination complex. The complex was characterized in MeOH solution by UV/vis/near-IR spectroscopy and in the solid state by single-crystal X-ray diffraction analysis. In the solid state, the complex exists as a 2 : 1 coordination complex, $[\text{Pu}(\mathbf{2})_2(\text{NO}_3)_3]^+[\text{Pu}(\text{NO}_3)_6]_{0.5}^{2-}$, with the two ligands (**2**) bonded to the Pu(IV) ion in a bidentate fashion. Six oxygen atoms from three bidentate nitrate ions also occupy inner-sphere coordination positions. The complex cation charge is balanced by a hexanitratoplutonium(IV) dianion that resides on an inversion center between two monocationic $[\text{Pu}(\mathbf{2})_2(\text{NO}_3)_3]^+$ units. The ten-vertex coordination polyhedron of the cation is distorted from square antiprismatic towards a sphenocorona. Optical absorbance spectra of the Pu(IV) in MeOH containing varying concentrations of nitrate and **2**, show that multiple complexes form in solution.

The coordination chemistry of d-block and 4f-block element ions has been actively studied over the last sixty years and much is known about the preferred inner-sphere coordination numbers and geometries as well as ligand affinities of these species. With the exception of Th(IV) and UO₂²⁺ ions, much less is known regarding the coordination preferences of 5f-block element ions.^{1–3} Consequently, for these ions it is much more difficult to model their behavior in environmental media or to design ligands that could serve as selective separation or detection agents. The lack of information stems, in part, from the radiation characteristics of the elements and the special handling conditions required to work with milligram quantities of materials. Driven by the increasing need to thoroughly understand the behavior of 5f element species under environmental conditions as well as in chemical separations/detection processes, efforts to expand the fundamental knowledge base on 5f element coordination chemistry have increased. In this regard, our group has recently reported the isolation and crystallographic characterization of $[\text{Pu}(\text{H}_2\text{O})_9][\text{CF}_3\text{SO}_3]_3$ as well as spectroscopic characterization of the species in the solid state and in 1 M triflic acid.⁴ This provided the first structural characterization of an aqueous molecular Pu(III) complex and it represents a “reference complex” for ligand design activities for Pu(III) now in progress. We have also reported the isolation and crystallographic characterization of $[\text{Pu}(\mathbf{1})_2(\text{NO}_3)_2](\text{NO}_3)_2$,⁵ a complex formed between Pu(IV) in nitric acid solution and the trifunctional ligand **1** (NOPOPO). These results are guiding further development of phosphinopyridine ligands as selective extractants.^{6–12} We report here the formation and crystal structure determination of a Pu(IV) complex with the bifunctional phosphinomethylpyridine *N,P*-dioxide ligand **2** (NOPO), and a discussion of the contrasts in coordination chemistry displayed by Pu(IV) and lanthanide ions which favor formation of $[\text{Ln}(\mathbf{2})_4]^{3+}$ species.⁹



Results and discussion

As noted above, we have previously reported that the sterically bulky trifunctional ligand **1** combines with $\text{Pu}(\text{NO}_3)_6^{2-}$ forming a 2 : 1 L : M complex $[\text{Pu}(\mathbf{1})_2(\text{NO}_3)_2](\text{NO}_3)_2$ in which the Pu(IV) ion binds with **1** in a tridentate chelate mode along with two distinctly asymmetric bidentate nitrate anions.⁵ In contrast, **2** is bifunctional and sterically less demanding. Hence Pu(IV) might be expected to coordinate more than two ligands. In fact, the lanthanide nitrates, $\text{Ln}(\text{NO}_3)_3$ (Ln = Pr, Tb and Yb), readily form not only bis-(ligand) complexes, $\text{Ln}(\mathbf{2})_2(\text{NO}_3)_3$, but, in the presence of excess **2**, they generate tetrakis-(ligand) complexes, $[\text{Ln}(\mathbf{2})_4](\text{NO}_3)_3$, in which **2** is bidentate and all nitrate ions appear in the outer-sphere.⁹

In the present study, a 1 : 1 L : M combination in 0.5 M HNO₃–EtOH solution produces orange–brown crystals that were analyzed by single-crystal X-ray diffraction methods.¹³ A view of the complex appears in Fig. 1 and selected bond distances and angles are summarized in Table 1. Clearly, in the solid state, the complex is not a simple 1 : 1 complex, $\text{Pu}(\mathbf{2})(\text{NO}_3)_4$. Instead, it consists of a cation, $[\text{Pu}(\mathbf{2})_2(\text{NO}_3)_3]^+$, that contains two bifunctional ligands **2** and three inner-sphere nitrate ions. A counter ion, $[\text{Pu}(\text{NO}_3)_6]_{0.5}^{2-}$, is located on an inversion center between two cations. The structure of the cation qualitatively resembles the structure of the 2 : 1 L : M lanthanide complex, $\text{Pr}(\mathbf{2})_2(\text{NO}_3)_3$.⁹ The ligands **2** are bonded to the Pu(IV) in a bidentate chelate mode with Pu–O(P), 2.309(3)

Table 1 Selected bond lengths [Å] and angles [°] for $[\text{Pu}(\text{NO}_3)_6]_{0.5}^-$

$[\text{Pu}(\text{NO}_3)_6]_{0.5}^-$			
Pu(1)–O(1)	2.334(4)	Pu(1)–O(2)	2.309(3)
Pu(1)–O(3)	2.344(4)	Pu(1)–O(4)	2.315(3)
Pu(1)–O(5)	2.582(4)	Pu(1)–O(6)	2.505(4)
Pu(1)–O(8)	2.463(4)	Pu(1)–O(9)	2.484(4)
Pu(1)–O(11)	2.446(4)	Pu(1)–O(12)	2.505(4)
P(1)–O(2)	1.505(4)	N(1)–O(1)	1.334(6)
P(2)–O(4)	1.498(4)	N(2)–O(3)	1.336(6)
O(2)–Pu(1)–O(1)	76.0(1)	O(2)–Pu(1)–O(4)	146.2(1)
O(4)–Pu(1)–O(1)	135.8(1)	O(2)–Pu(1)–O(3)	72.8(1)
O(4)–Pu(1)–O(3)	75.9(1)	O(1)–Pu(1)–O(3)	148.3(1)
O(2)–Pu(1)–O(11)	72.4(1)	O(4)–Pu(1)–O(11)	120.6(1)
O(1)–Pu(1)–O(11)	74.6(2)	O(3)–Pu(1)–O(11)	90.7(2)
O(2)–Pu(1)–O(8)	140.4(1)	O(4)–Pu(1)–O(8)	71.7(1)
O(1)–Pu(1)–O(8)	73.5(1)	O(3)–Pu(1)–O(8)	130.7(1)
O(11)–Pu(1)–O(8)	75.6(2)	O(2)–Pu(1)–O(9)	134.1(1)
O(4)–Pu(1)–O(9)	69.4(1)	O(1)–Pu(1)–O(9)	67.9(1)
O(3)–Pu(1)–O(9)	141.3(1)	O(11)–Pu(1)–O(9)	121.2(2)
O(8)–Pu(1)–O(9)	51.5(2)	O(2)–Pu(1)–O(12)	130.7(1)
O(4)–Pu(1)–O(12)	70.4(1)	O(1)–Pu(1)–O(12)	117.1(1)
O(3)–Pu(1)–O(12)	69.3(1)	O(11)–Pu(1)–O(12)	51.0(1)
O(8)–Pu(1)–O(12)	65.3(2)	O(9)–Pu(1)–O(12)	112.3(2)
O(2)–Pu(1)–O(6)	84.2(1)	O(4)–Pu(1)–O(6)	71.9(1)
O(1)–Pu(1)–O(6)	115.7(1)	O(3)–Pu(1)–O(6)	66.6(1)
O(11)–Pu(1)–O(6)	151.6(2)	O(8)–Pu(1)–O(6)	131.9(1)
O(9)–Pu(1)–O(6)	86.6(2)	O(12)–Pu(1)–O(6)	127.2(1)
O(2)–Pu(1)–O(5)	73.2(1)	O(4)–Pu(1)–O(5)	106.0(1)
O(1)–Pu(1)–O(5)	66.4(1)	O(3)–Pu(1)–O(5)	108.8(1)
O(11)–Pu(1)–O(5)	132.8(1)	O(8)–Pu(1)–O(5)	115.2(2)
O(9)–Pu(1)–O(5)	66.9(2)	O(12)–Pu(1)–O(5)	176.1(1)
O(6)–Pu(1)–O(5)	49.3(1)		
$[\text{Pu}(\text{NO}_3)_6]_{0.5}^{2-}$			
Pu(2)–O(14)	2.492(4)	Pu(2)–O(15)	2.533(4)
Pu(2)–O(17)	2.460(4)	Pu(2)–O(18)	2.476(5)
Pu(2)–O(20)	2.495(5)	Pu(2)–O(21)	2.482(5)

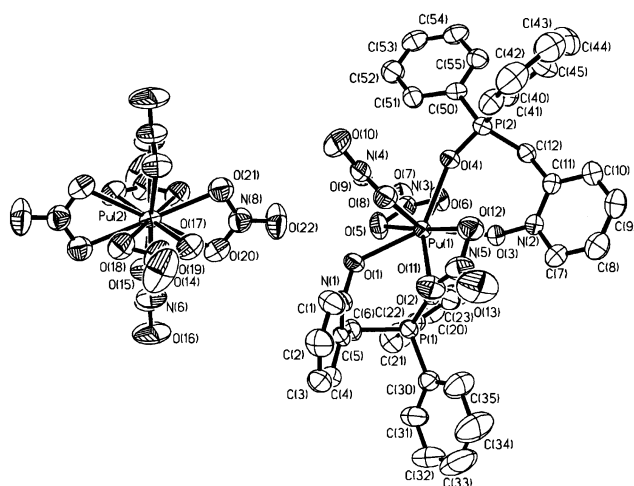


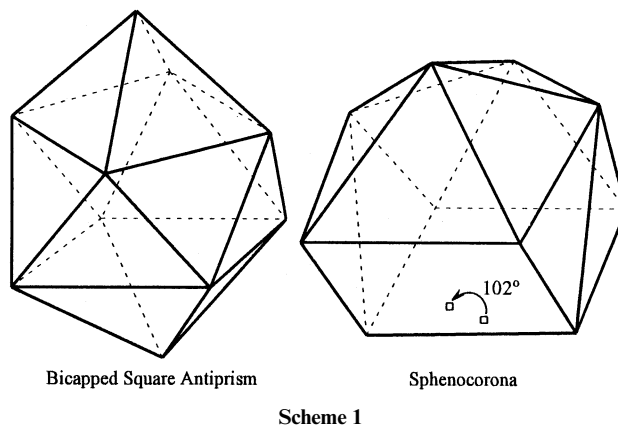
Fig. 1 Thermal ellipsoid plot (40%) of $[\text{Pu}(\text{NOPOPO})_2(\text{NO}_3)_3]^+[\text{Pu}(\text{NO}_3)_6]_{0.5}^-$.

Å, and 2.315(3) Å (av. 2.312 Å), and Pu–O(N), 2.344(4) Å and 2.334(4) Å (av. 2.339 Å). These distances are shorter than the corresponding average distances in the Pr(III) complex: Pr–O(P) 2.456(6) Å and Pr–O(N) 2.445(7) Å. This is to be expected since Pr(III) is significantly larger than Pu(IV).¹⁴ It is also interesting that the Pu–O(P) distances are shorter than the Pu–O(N) distances in $[\text{Pu}(\text{NOPOPO})_2(\text{NO}_3)_3]^+$ while the Pr–O(P) and Pr–O(N) distances are identical, within 2σ of the e.s.d.s, in $\text{Pr}(\text{NO}_3)_3$. Based upon these data alone, one might conclude that the more polarizing Pu(IV) ion is resolving a difference in donor strength between the P=O and N–O groups in **2**. In contrast, for $[\text{Pu}(\text{NOPOPO})_2(\text{NO}_3)_3]^+$ there is a larger range of Pu–O(P) distances, 2.310(4) Å to 2.382(4) Å, and the average distances, Pu–O(P)

2.347(4) Å and Pu–O(N) 2.342(4) Å are identical. In this complex, ligand steric and packing effects are also affecting the Pu(IV)/2 coordinate bond distances. Although ligand–ligand steric congestion is much less in the $[\text{Pu}(\text{NOPOPO})_2(\text{NO}_3)_3]^+$ cation, it is premature to conclude that, toward Pu(IV), the P=O group in **2** is a stronger donor than the N–O group based upon the metal–oxygen bond length data.

The ten-vertex inner-sphere coordination polyhedron for $[\text{Pu}(\text{NOPOPO})_2(\text{NO}_3)_3]^+$ has been described as a bicapped square antiprism.⁵ The two capping oxygen atoms in that structure display long Pu–O distances, 2.710(5) Å and 2.824(5) Å, that belong to two asymmetrically bound nitrate groups. In contrast, the ten-vertex polyhedron of $[\text{Pu}(\text{NOPOPO})_2(\text{NO}_3)_3]^+$ does not have long Pu–O(nitrate) interactions, and the coordination polyhedron does not resemble an ideal bicapped-square antiprism. The bidentate nitrate ions are bound to the Pu(IV) in a more symmetric fashion, and the Pu–O (nitrate) distances have a small range, 2.446(4) Å to 2.582(4) Å. These parameters are comparable to the Pu–O distances found in the hexanitrate anion in the current structure, 2.460(4) Å to 2.533(4) Å, and in the structure of its bis-ammonium salt,¹⁵ 2.454(6) Å to 2.516(5) Å.

Based upon repulsion models for ten-coordinate molecules,¹⁶ the two most favored idealized ten-vertex polyhedra are the bicapped square antiprism and the sphenocorona as shown in Scheme 1. The bicapped square antiprism is defined by the two



parallel square faces of the antiprism and a 180° angle between the two bonds of the capping atoms. The sphenocorona is characterized by two planar, trapezoidal faces meeting at an angle of approximately 102° . Fig. 2 shows the observed coordination

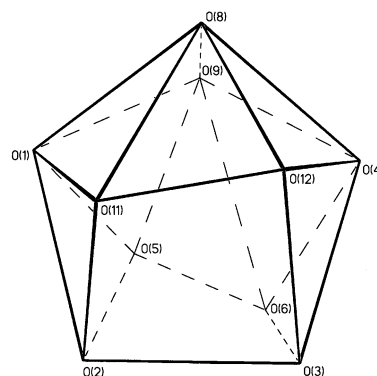


Fig. 2 Coordination polyhedron displayed in the $[\text{Pu}(\text{NOPOPO})_2(\text{NO}_3)_3]^+$ cation.

sphere for the cation unit of $[\text{Pu}(\text{NOPOPO})_2(\text{NO}_3)_3]^+[\text{Pu}(\text{NO}_3)_6]_{0.5}^-$. The best arrangement for a bicapped square antiprism would have O(5) and O(12) as the capping atoms. The O(5)–Pu(1)–O(12) angle in this case is $176.1(1)^\circ$. However, the planes defined by O(11), O(8), O(4), O(3) and O(1), O(6), O(2), O(9)

deviate from planarity by 0.087 Å and 0.196 Å, respectively. The dihedral angle between these planes is 3.4°, as compared with 0.9° in the Pu(IV) structure containing ligand **1**.⁵ The alternative ideal polyhedron, described as a sphenocorona, can be considered to contain two trapezoidal planes defined by the atoms O(2), O(3), O(11), O(12), and O(2), O(3), O(5), O(6); the angle between the planes is 109.5°, which deviates somewhat from the ideal angle of 102°. Hence, the observed inner-sphere polyhedron is not exactly described by either idealized ten-vertex polyhedron. Instead it resides somewhere in-between.

Plutonium(IV) in acidic solution generally undergoes rapid ligand exchange and its speciation is complicated. Given the diversity of the system described here, with multiple potential ligands including water, methanol, nitrate and P=O and N–O donor groups and the variable ligand denticities for NO₃[−] and **2**, it is likely that aqueous and alcoholic solutions contain multiple species. This speciation was investigated using UV/vis/near-IR spectroscopy. Fig. 3 shows spectra of Pu(IV) (5.0 mM)

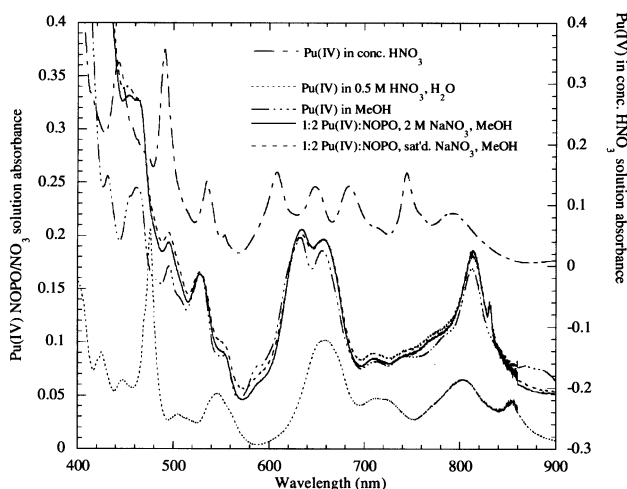


Fig. 3 UV/vis absorbance spectra of 5.0 mM Pu(IV) in MeOH and 2.5 mM Pu, 5.0 mM NOPO in 1 : 1 MeOH : H₂O with varying [NaNO₃].

in MeOH and of Pu(IV) in MeOH solutions containing **2** (1 : 2 Pu(IV) : **2**) and NaNO₃ [2 M and satd. (≈4 M)]. The similarity of these spectra suggest that the Pu(IV) chromophore in MeOH solution is not strongly perturbed by the addition of NO₃[−] up to a ≈1 : 1000 Pu : NO₃[−] ratio. This further suggests that NO₃[−] ions do not dominate the inner-sphere coordination environment of Pu(IV) in MeOH. Fig. 3 also contains spectra of Pu(IV) in water (0.5 M HNO₃) and in concentrated nitric acid.¹⁷ These spectra differ from each other, from the MeOH solution spectra and from the diffuse reflectance spectra for several isolated salts containing the Pu(NO₃)₆^{2−} ion.¹⁸ These observations imply that MeOH and H₂O both act as solvating ligands even in the presence of 2–4 M nitrate. Under no condition studied here is Pu(NO₃)₆^{2−} observed in solution.¹⁹

In order to further probe the speciation of the Pu(IV)/NO₃[−]/**2** system in MeOH, a titration was performed in which aliquots of Pu(IV) stock solution were added to a 5.0 mM solution of **2** in MeOH. The spectra of the resulting solutions are shown in Fig. 4.²⁰ Three isosbestic points appear at ≈530, 580 and 640 nm consistent with the existence of two or more species in these solutions. In addition, as the ligand concentration increases relative to Pu(IV) there are significant red-shifts in the λ_{max} of several prominent absorptions and a change in band shape in the region 600–700 nm. This is consistent with progressive displacement of MeOH and/or H₂O from the Pu(IV) inner-sphere by **2** as the amount of **2** is increased.

The diffuse reflectance spectrum for the complex [Pu(**2**)₂(NO₃)₃]⁺[Pu(NO₃)₆^{2−}]_{0.5} was not obtained although it would be expected to be complicated due to the presence of not only the cation containing **2**, but also the [Pu(NO₃)₆^{2−}] anion. Since the

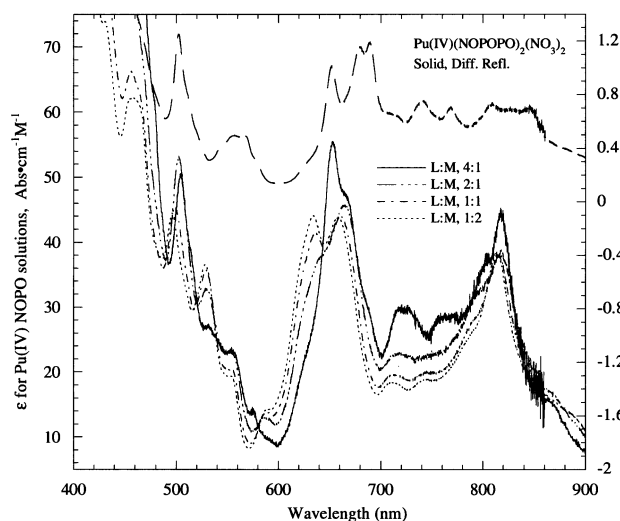


Fig. 4 UV/vis absorbance spectra of [Pu(NOPO)₂(NO₃)₃][Pu(NO₃)₆]_{0.5} in MeCN, [Pu(NOPOPO)₂(NO₃)₂](NO₃)₂ in MeOH, Pu(IV) nitric acid diluted in MeOH; UV/vis diffuse reflectance spectrum of solid [Pu(**1**)₂(NO₃)₂](NO₃)₂.

solution spectra of the complex do not display absorptions that have been previously attributed to [Pu(NO₃)₆^{2−}],¹⁸ we might speculate that the solution spectra of mixtures with 1 : 1 and 2 : 1 L : Pu ratios might more resemble the spectrum of [Pu(**1**)₂(NO₃)₂]²⁺(NO₃)₂ reported previously.⁵ These spectra are presented in Fig. 5 along with the spectrum of Pu(IV)/HNO₃

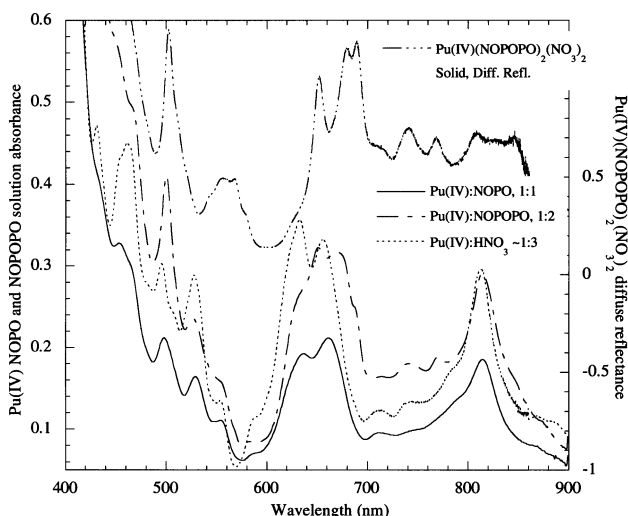


Fig. 5 UV/vis absorbance spectra of Pu(IV) NOPO complexes in MeOH at 5.0 mM NOPO and varying ligand to metal ratios. A spectrum of the Pu(IV) HNO₃ stock solution diluted in MeOH to yield 5 mM Pu is also shown for comparison. (All spectra are plotted in terms of molar absorptivities.)

(1 : 3) in MeOH and the diffuse reflectance spectrum for the [Pu(**1**)₂(NO₃)₂]²⁺(NO₃)₂ complex. Once again, the prominent absorptions in the solution and solid spectra containing **1** and **2** are red-shifted relative to the Pu(IV)/MeOH solution. This is consistent with **1** and **2** displacing MeOH from the Pu(IV) inner-sphere. Further conclusions regarding speciation in solution must await additional more extensive studies with these and other related ligands.

Experimental

The ligand, 2-[(diphenylphosphino)methyl]pyridine *N,P*-dioxide (**2**), was prepared according to the published procedure.¹⁰ Standard radiochemical procedures were used for the synthesis of Pu complexes. All the manipulations were

performed in either HEPA-filtered fume hoods or negative pressure glove boxes. Acetonitrile, methanol and ethanol were obtained from J. T. Baker and were used without purification. Distilled water was used for all aqueous and mixed-solvent solution preparations. Plutonium-239 stock solutions were prepared as described in the literature.^{21,22} The solutions were purified with an anion exchange resin (Lewatite MP-500) that binds Pu(IV) as an anionic nitrate complex. The Pu(IV) was eluted with 0.5 M HNO₃. The stock solutions were assayed using UV/vis/near-IR spectroscopy to verify the oxidation state purity and solution concentration. The Pu(IV) oxidation state was confirmed and plutonium content assayed by using a characteristic absorbance band at 470 nm ($\epsilon = 58 \text{ M}^{-1} \text{ cm}^{-1}$).^{22–25}

Preparation of $[\text{Pu}(\mathbf{2})_2(\text{NO}_3)_3]^+[\text{Pu}(\text{NO}_3)_6]^{2-}]_{0.5}$

The complex was prepared by adding a 100 μL aliquot of a 0.17 M solution of $\text{Pu}(\text{NO}_3)_6^{2-}$ in 0.5 M HNO₃ to $\mathbf{2}$ (0.0089 g, 17.0 μmol) dissolved in ethanol (1 mL). Upon addition to the ligand, the Pu(IV) solution turned orange–brown. The solution volume was evaporated by half and the vial was capped. Orange–brown X-ray quality crystals formed after a few days. Crystals were dissolved in acetonitrile to obtain the optical absorbance spectrum, shown in Fig. 5.

Optical spectra

HPLC grade methanol and ACS grade sodium nitrate were obtained from Fisher and used without purification. Plutonium(IV)/5.0 mM $\mathbf{2}$ solutions with varying metal to ligand ratios were prepared by dissolving 15.5 mg of $\mathbf{2}$ (FW = 309.3 g mol⁻¹) in methanol and sequentially adding appropriate volumes of a 0.318 M Pu, 1.0 M HNO₃ stock solution. Methanolic solutions of Pu(IV) and $\mathbf{2}$ alone were prepared by adding appropriate volumes of the Pu stock solution or appropriate masses of the phosphine oxide solid, respectively, to 1.0 or 2.0 mL methanol. Methanol/water solutions of Pu(IV), $\mathbf{2}$, and NaNO₃ were prepared similarly, where the ligand was dissolved in methanol, then an appropriate amount of the Pu(IV)/nitric acid stock solution was added, and then solid NaNO₃ was added. Equal volumes of water were added to dissolve the NaNO₃. Final solution concentrations were 5 mM $\mathbf{2}$, 2.5 mM Pu(IV), ≈ 0.8 mM HNO₃ and either 2.0 M or saturated (≈ 4 M) NaNO₃. Optical absorbance spectra were obtained using a Cary 500 (Varian) spectrophotometer. The diffuse reflectance spectrum of $[\text{Pu}(\mathbf{1})_2(\text{NO}_3)_2](\text{NO}_3)_2$ was measured using a Perkin-Elmer Lambda 9 spectrophotometer and was previously reported.⁵

Crystallographic analysis

Suitable crystals were selected from samples prepared as described above and coated with a thin protective film of epoxy. The coated crystals were then sealed in glass capillaries that were coated on the outside with acrylic to provide structural stability to the capillaries and multiple containment of the radioactive material. The crystals were screened for maximum scattered intensity and the best crystal was utilized for data collection. Selected crystallographic data for the complex are presented in Table 2. Diffraction data were collected at ambient temperature on a Bruker P4/PC diffractometer equipped with a CCD area detector by using both ϕ and ω scan methods; a full hemisphere of data was collected. The program SADABS²⁶ was used to correct for absorption and decay. The structure was solved by Patterson and difference Fourier methods with the program SHELXS-97.²⁷ The light non-hydrogen atoms were located by least-squares refinement and subsequent difference Fourier analysis using SHELXL-97.²⁸ All non-hydrogen atoms were refined anisotropically to convergence. Refinement on F^2 , for 628 parameters and 6115 unique reflections, gave $R1 = 0.0256$, $wR2 = 0.0601$.

Table 2 Selected crystallographic data

Formula	C ₃₆ H ₃₂ N ₈ O ₂₂ P ₂ Pu _{1.5}
M	1353.64
Crystal system	Triclinic
Space group	$P\bar{1}$
$a/\text{\AA}$	12.0407(6)
$b/\text{\AA}$	14.2228(7)
$c/\text{\AA}$	15.6363(7)
a°	65.195(1)
β°	80.571(1)
γ°	72.381(1)
$U/\text{\AA}^3$	2314.6(2)
Z	2
$D_c/\text{g cm}^{-3}$	1.942
T/K	293
$\lambda/\text{\AA}$	0.71073
μ/mm^{-1}	2.283
$R1 [I > 2\sigma(I)]$	0.0256 ^a
$wR2^b$	0.0601 ^b
GOF	1.065

^a $R1 = \sum ||F_o| - |F_c|| / \sum |F_o|$. ^b $wR2 = [\sum w(|F_o| - |F_c|)^2] / \sum [w(F_o^2)^2]^{1/2}$; $w = 1/[\sigma^2(F_o^2) + (aP)^2 + bP]$; $P = [\max(F_o^2 \text{ or } 0) + 2(F_c^2)]/3$.

CCDC reference number 174541.

See <http://www.rsc.org/suppdata/dt/b1/b106624m/> for crystallographic data in CIF or other electronic format.

Acknowledgements

R. T. P. thanks the U.S. Department of Energy, Office of Basic Energy Sciences (Grant DE-FG03-94ER14446) for financial support of the ligand development research at UNM. This work on actinide complexation was performed under the auspices of the Chemical Sciences Division, Office of Science, Office of Basic Energy Sciences, of the U.S. Department of Energy. Los Alamos National Laboratory is operated by the University of California for the U.S. Department of Energy under contract W-7405-ENG-36. The authors also thank Mr Sean Reilly for preparing some of the Pu stock solutions and Dr John Berg and Mr Phil Palmer for providing the spectrum of hexanitratoplutonium(IV) in concentrated HNO₃.

References and notes

- J. Katz, G. T. Seaborg and L. Morss, *The Chemistry of the Actinide Elements*, 2nd edn., Longman, London, 1986.
- G. T. Seaborg and W. D. Loveland, *The Elements Beyond Uranium*, Wiley-Interscience, New York, 1990.
- Handbook on the Physics and Chemistry of Rare Earths, Vol 18 – Lanthanides and Actinides Chemistry*, K. A. Gschneidner, Jr., L. Eyring, G. R. Choppin and G. H. Lander, eds., Elsevier Science, New York, 1994.
- J. H. Matonic, B. L. Scott and M. P. Neu, *Inorg. Chem.*, 2001, **40**, 2638–2640.
- E. M. Bond, E. N. Duesler, R. T. Paine, M. P. Neu, J. H. Matonic and B. L. Scott, *Inorg. Chem.*, 2000, **39**, 4152.
- E. M. Bond, U. Engelhardt, T. P. Deere, B. M. Rapko, R. T. Paine and J. R. FitzPatrick, *Solv. Extract. Ion Exch.*, 1997, **15**, 381.
- E. M. Bond, U. Engelhardt, T. P. Deere, B. M. Rapko, R. T. Paine and J. R. FitzPatrick, *Solv. Extract. Ion Exch.*, 1998, **16**, 967.
- K. L. Nash, D. D. Ensor, X. M. Gan and R. T. Paine, unpublished work.
- B. M. Rapko, E. N. Duesler, P. H. Smith, R. T. Paine and R. R. Ryan, *Inorg. Chem.*, 1993, **32**, 2164.
- U. Engelhardt, B. M. Rapko, E. N. Duesler, D. Frutos, R. T. Paine and P. H. Smith, *Polyhedron*, 1995, **14**, 2361.
- E. M. Bond, X. Gan, J. R. FitzPatrick and R. T. Paine, *J. Alloys Compds.*, 1998, **271–273**, 172–175.
- X. Gan, E. N. Duesler, R. T. Paine and P. H. Smith, *Inorg. Chim. Acta*, 1996, **247**, 29.
- The 2 : 1 and 4 : 1 L : M combinations were also examined. At this time crystals obtained from the 2 : 1 mixture are badly twinned so the structure remains unknown. The complex formed from the 4 : 1 mixture displays significantly different features in the UV/vis/

- near-IR spectrum that suggest a different coordination environment for Pu(IV).
- 14 R. D. Shannon and C. T. Prewitt, *Acta Crystallogr., Sect. B*, 1969, **25**, 925–946. Values of the ionic radius for Pu(IV) and Pr(III) with coordination number (CN) = 10 are not provided so the values for CN = 8 have been used: Pr(III) (CN = 8) $r = 1.14 \text{ \AA}$; Pu(IV) (CN = 8) $r = 0.96 \text{ \AA}$.
 - 15 M. R. Spirlet, J. Rebizant, C. Apostolidis, B. Kanellakopulos and E. Dornberger, *Acta Crystallogr., Sect. C*, 1992, **48**, 1161.
 - 16 D. L. Kepert, *Inorganic Stereochemistry*, Springer Verlag, Berlin, 1982, p. 188.
 - 17 In companion experiments, UV/vis/near-IR spectra recorded from solutions containing 5 mM Pu(IV) in aqueous HNO₃ (2 M, 4 M) are identical to the spectrum shown in Fig. 3 for Pu(IV) in aqueous 0.5 M HNO₃.
 - 18 Diffuse reflectance spectra of solid samples of the hydronium salt [H₃O⁺ 18-Crown-6]₂[Pu(NO₃)₆²⁻] and the tetrabutylammonium salt [N(*n*-Bu)₄⁺]₂[Pu(NO₃)₆²⁻] are essentially identical in the visible region. Principal absorption bands are observed at 438, 457, 484, 529, 600 and 635 nm. Similar spectra were also obtained for solid samples of both the caesium and ammonium salts of the hexanitratoplutonium dianion, Cs₂[Pu(NO₃)₆] and [NH₄⁺]₂[Pu(NO₃)₆²⁻], respectively: P. L. Gordon, D. W. Keogh, P. D. Palmer and C. D. Tait, unpublished work.
 - 19 This observation is consistent with Pu(NO₃)₆²⁻ forming only in very concentrated nitrate solutions: P. G. Allen, D. K. Veirs, S. D. Conradson, C. A. Smith and S. F. Marsh, *Inorg. Chem.*, 1996, **35**, 2841; D. K. Veirs, C. A. Smith, J. M. Berg, B. D. Zwick, S. F. Marsh, P. G. Allen and S. D. Conradson, *J. Alloys Compds.*, 1994, **213**, 328.
 - 20 The UV/visible spectrum of CHCl₃ or MeOH solutions of **2** show no absorption bands in the region 300–900 nm.
 - 21 J. L. Ryan, *J. Phys. Chem.*, 1960, **64**, 1375.
 - 22 (a) J. L. Ryan and E. J. Wheelwright, *The Recovery, Purification, and Concentration of Plutonium by Anion Exchange in Nitric Acid* General Electric Company Hanford Atomic Products Operations report HW-55893, January 1959; (b) J. P. Faris and R. F. Buchanan, *Applications of Anion Exchange Chromatographic Procedures in Nitric Acid Medium* U.S. Atomic Energy Commission report TID-7606, pp. 185–194, 1960; (c) R. W. Durham and R. Mills, *The Adsorption of Plutonium on Anion Resins*, Atomic Energy of Canada Ltd., report CEI-62, 1953.
 - 23 W. P. Carey and L. E. Wangen, *Chemom. Intell. Lab. Syst.*, 1991, **10**, 245.
 - 24 M. Eiswirth, J. I. Kim and C. Lierse, *Radiochim. Acta*, 1985, **38**, 197.
 - 25 H. Capdevila, P. Vitorge, E. Giffaut and L. Delmau, *Radiochim. Acta*, 1996, **74**, 93.
 - 26 G. M. Sheldrick, Empirical Absorption Correction Program, Universität Göttingen, 1996.
 - 27 G. M. Sheldrick, Program for Crystal Structure Solution, Universität Göttingen, 1997.
 - 28 G. M. Sheldrick, Program for Crystal Structure Refinement, Universität Göttingen, 1997.